Application of Adaptive Least-Squares Algorithm to Multi-Element Array Signal Reconstruction

R. Kumar
Communications Systems Research Section

This article presents some results in terms of the performance improvement of a multi-feed array configuration over the usual single feed system when an adaptive least-squares algorithm is applied for the signal reconstruction. The article presents two novel versions of the least-squares algorithm, one of which is based on the maximization of the signal-to-noise ratio while the other is based on the deconvolution of the received signal field. These algorithms have been developed for the purpose of minimizing degradations arising from various sources, which can severely limit the performance (gain) of a single-feed system.

I. Introduction

The development of multi-element array processing techniques has many potential applications for the Deep Space Network (DSN). These include signal reconstruction for both X-band and Ka-band communications [1–4] and electronic pointing to augment existing mechanical pointing techniques. For all of these applications, multi-element array processing can generally provide significant performance improvements over single-feed antenna configurations, which are predominantly used in the DSN.

This article presents some results in terms of the performance improvement provided by a linear multi-feed array incorporating the proposed adaptive least-squares algorithm over a single-feed array system, as applied to the signal reconstruction problem. While the assumed linear array geometry is idealized, the results of this analysis provide an indication of performance improvements that can be achieved with adaptive, multi-element array processing. This article describes two versions of the least-squares algorithm, one of which is based on the maximization of the signal-to-noise ratio while the other is based on deconvolution of the received signal field. Here, instead of trying to model the signal degradations in terms of deterministic equations in evaluating the performance of the algorithm, it is assumed that these degradations are "unknown" to the algorithm and vary with time. The algorithm tries to implicitly estimate these degradations in an adaptive manner from the samples of the noisy received signal. On the basis of these measurements, it computes a set of weights for combining signals at the outputs of various feeds in order to maximize the signal-to-noise ratio of the combined signal.

For the purposes of illustrating the basic concepts involved with adaptive array processing, this article presents

the results for a 16-element linear-array feed system. The performance of the least-squares algorithm is to a first order determined by the signal-to-noise ratio of the received signal, the number of feeds in the configuration, and the time constants at which the received signal field is varying with time.

In practice, it may be possible to simultaneously correct for multiple degradations arising from different sources and having different time constants. These degradations may be induced by wind, gravitational loading, or antenna pointing errors. Simultaneous correction for such degradations could be achieved by adjusting the time constants of the algorithm to track the fastest mode, in which case the slower modes would be estimated sub-optimally. Alternatively, one could track the most significant mode, thereby essentially ignoring the faster but less significant modes. More sophisticated techniques could also be used for separation of the modes and tracking of them separately.

II. Array Configuration

The specific array configuration of interest in this article corresponds to a linear-feed array distributed across the focal plane of an antenna. The array outputs are then fed to a parallel receiver bank as indicated in Fig. 1. As shown in the schematic diagram of Fig. 1, the signal outputs from the feed elements are amplified by r f amplifiers. Assuming that all of the amplifiers have equal gain and noise temperature, the output of the ith amplifier can be written as

$$r_i(t) = A_i(t)\cos\Big(\omega_c t + \theta_i(t)\Big) + n_i(t) \qquad (1)$$

where $A_i(t)$ and $\theta_i(t)$ are the signal amplitudes and phases, ω_c denotes the signal carrier frequency, and $n_i(t)$ is a zero-mean white Gaussian noise of one-sided spectral density N_0. The noise is also assumed to be spatially uncorrelated, i.e., $E\left[n_i(t)n_j(t)\right] = 0$ for $i \neq j$ and $i, j = 1, 2, .., N$. Under ideal conditions and assuming a plane-wave normally incident on the antenna aperture, the amplitude of the center feed would be equal to $\sqrt{2P}$ (P denotes the normalized power received by the antenna), while the remaining feeds will have nearly zero amplitude. However, array degradations can disperse the signal amplitude (and phase) spatially over N feeds. These degradations can arise due to various sources, such as gravity, thermal fields, wind, and atmospheric turbulence.

In the presence of such degradations, the adaptive signal processing algorithm then combines the N feed outputs in a coherent manner so as to optimise some performance index, such as the signal-to-noise power ratio of the combined signal. This processing can occur either at r f or can be equivalently done at the baseband. Alternatively, in some possible imaging applications, it may be desired to reconstruct the complete focal plane field, i.e., obtain N output signals that are close to the outputs of the focal plane fields in the ideal antenna case.[1] Note that in the more general case, more than one feed may have significant amplitude if the source is not a point source and the antenna is capable of resolving such a composite source. In the limiting case, one may simply use the center output of the reconstructed field and ignore the others, thus achieving an alternative combination of the input signals.

For the purposes of signal processing, the N received r f signals $r_i(t)$; $i = 1, 2, ..., N$ are down-converted and quadrature sampled to obtain the sampled version of the complex baseband envelope $g_i(t)$ of the r f signal $r_i(t)$ with

$$\begin{aligned} r_i(t) &= Re\Big\{g_i(t)e^{j\omega_c t}\Big\} \\ g_i(t) &= A_i(t)e^{j\theta_i(t)} + \nu_i(t) \qquad (2) \\ g_i(t) &= \Big\{r_i(t) + \hat{r}_i(t)\Big\}e^{-j\omega_c t} \end{aligned}$$

In Eq. (2) above, $\hat{r}_i(t)$ denotes the Hilbert transform of $r_i(t)$, and $\nu_i(t)$ is the complex envelope of the bandpass noise $n_i(t)$.

III. Signal Combining Via Adaptive Least-Squares Algorithm I

As shown in Fig. 1, the adaptive algorithm determines the time-varying complex-valued weighting coefficients $w_1(k), ..., w_N(k)$ on the basis of signal samples $g_i(j)$; $i = 1, 2, ..., N$; and $j = 1, 2, ..., k$ according to some appropriate optimization criterion. The algorithm is adaptive in the sense that if the signal amplitudes and phases (A_i and θ_i) remain relatively constant with time, then with increasing value of k, the algorithm achieves increasingly accurate estimates of these parameters, and the weighting coefficients converge asymptotically to their theoretically optimum values with an exponential convergence rate. On the other hand, if these parameters are time-varying, then

[1] V. Vilnrotter, "Ka-Band Array Signal Processing Progress Report," JPL Interoffice Memorandum No. 331-88.5-047 (internal document), Jet Propulsion Laboratory, Pasadena, California, November 1988.

the algorithm tracks these variations and the weighting coefficients are truly time-varying (there is no tendency for $w_i(k)$ to converge to some constant value).

Denoting by $\underline{w}(k)$ and $\underline{g}(k)$ the weighting coefficient vector $[w_1(k)w_2(k)\ldots w_N(k)]'$ and the measurement vector $[g_1(k)g_2(k)\ldots g_N(k)]'$ respectively, then the familiar least-square optimization criterion is to select $\underline{w}(k)$ so as to minimize the following index

$$J_k = \sum_{j=1}^{k} |1 - \underline{w}^H(k)\underline{g}(j)|^2 \tag{3}$$

with respect to the weight vector $\underline{w}(k)$ for $k = 1, 2, \ldots$. In the above, the superscript H denotes conjugate transpose while $'$ represents just the transpose of a matrix. The optimal solution, termed least-squares estimate of $w(k)$, is given by (assuming $k > N$)

$$\underline{\hat{w}}_{LS}(k) = \left\{\sum_{j=1}^{k} \underline{g}(j)\underline{g}^H(j)\right\}^{-1} \sum_{j=1}^{k} \underline{g}(j) \tag{4}$$

If the distortion process is time-varying, then it is more appropriate to replace the index J_k by the one obtained by multiplying the summand in Eq. (3) by λ^{k-j} for some $0 < \lambda < 1$, minimization of which yields the following exponentially data-weighted least-squares estimate for $\underline{w}(k)$.

$$\underline{\hat{w}}_{ELS}(k) = \left\{\sum_{j=1}^{k} \lambda^{k-j}\underline{g}(j)\underline{g}^H(j)\right\}^{-1} \sum_{j=1}^{k} \lambda^{k-j}\underline{g}(j) \tag{5}$$

Note that in the adaptive algorithm's present non-recursive form, Eq. (4), it is required to invert an $(N \times N)$ matrix for every time instance k in the computation of $\hat{w}(k)$, which is somewhat computationally intensive. This problem can be overcome by replacing the estimate in Eq. (5) with its recursive form, which is obtained as follows.

Denoting by $\underline{P}(k)$ the matrix inverse in Eq. (5), then the matrix $\underline{P}^{-1}(k)$ has the following update.

$$\underline{P}^{-1}(k) = \lambda\underline{P}^{-1}(k-1) + \underline{g}(k)\underline{g}^H(k); \quad k = 1, 2, \ldots \tag{6}$$

Application of the matrix inversion lemma [5] to Eq. (6) yields the following desired recursion for $\underline{P}(k)$.

$$\underline{P}(k) = \lambda^{-1}\Big\{\underline{P}(k-1) - \left[\lambda + \underline{g}^H(k)\underline{P}(k-1)\underline{g}(k)\right]^{-1} \times \underline{P}(k-1)\underline{g}(k)\underline{g}^H(k)\underline{P}(k-1)\Big\} \tag{7}$$

One may note that the entity to be inverted in Eq. (7) is only a scalar. Decomposing the sum in Eq. (5) as

$$\lambda\sum_{j=1}^{k-1} \underline{g}(j)\lambda^{k-1-j} + \underline{g}(k)$$

and substituting Eq. (7) for $\underline{P}(k)$, we obtain the following expression for $\underline{\hat{w}}_{ELS}(k)$.

$$\begin{aligned}\underline{\hat{w}}_{ELS}(k) = \underline{P}(k-1) &\left\{\sum_{j=1}^{k-1} \underline{g}(j)\lambda^{k-1-j}\right\} \\ &- \left[\lambda + \underline{g}^H(k)\underline{P}(k-1)\underline{g}(k)\right]^{-1} \\ &\times \underline{P}(k-1)\underline{g}(k)\underline{g}^H(k)\underline{P}(k-1) \\ &\times \left\{\sum_{j=1}^{k-1} \lambda^{k-1-j}\underline{g}(j)\right\} + \underline{P}(k)\underline{g}(k)\end{aligned} \tag{8}$$

By noting that the first term in Eq. (8) and the product of the last two factors in the second term both are equal to $\underline{\hat{w}}_{ELS}(k-1)$, Eq. (8) may be rewritten as

$$\begin{aligned}\underline{\hat{w}}_{ELS}(k) = \underline{\hat{w}}_{ELS}(k-1) &+ \underline{P}(k)\underline{g}(k) \\ &- \left[\lambda + \underline{g}^H(k)\underline{P}(k-1)\underline{g}(k)\right]^{-1} \\ &\times \underline{P}(k-1)\underline{g}(k)\underline{g}^H(k)\underline{\hat{w}}_{ELS}(k-1)\end{aligned} \tag{9}$$

Post multiplying both sides of Eq. (7) by $\underline{g}(k)$ and with a simple algebraic manipulation, it follows that,

$$\left[\lambda + \underline{g}^H(k)\underline{P}(k-1)\underline{g}(k)\right]^{-1} \underline{P}(k-1)\underline{g}(k) = \underline{P}(k)\underline{g}(k) \tag{10}$$

With the substitution of Eq. (10) in the last term of Eq. (9), one obtains the recursive version of the algorithm given below.

$$\begin{aligned}\underline{\hat{w}}_{ELS}(k) &= \underline{\hat{w}}_{ELS}(k-1) + \underline{P}(k)\underline{g}(k) \\ &\quad \times \left[1 - \underline{g}^H(k)\underline{\hat{w}}_{ELS}(k-1)\right] \qquad (11) \\ \underline{P}(k) &= \lambda^{-1}\Big\{\underline{P}(k-1) - \left[\lambda + \underline{g}^H(k)\underline{P}(k-1)\underline{g}(k)\right]^{-1} \\ &\quad \times \underline{P}(k-1)\underline{g}(k)\underline{g}^H(k)\underline{P}(k-1)\Big\}; \\ &\quad k = 0, 1, 2, \ldots\end{aligned}$$

If the complex field $\underline{g}(k)$ is a wide-sense stationary process, a considerable simplification in computations may be achieved by replacing $\underline{P}(k)$ with an appropriate constant matrix in the first recursion of Eq. (11) and dropping the second recursion.

IV. Maximization of Signal-to-Noise Ratio via Modified Least-Squares Algorithm I

In some applications, it may be more appropriate to maximize the signal-to-noise power ratio at the combiner output. The noise variance at the output of the combiner is equal to $\sum_{i=1}^{N} |\hat{w}_i|^2 E[|\nu_i|^2] = \sigma^2 \|\underline{\hat{w}}\|^2$ with σ^2 denoting the variance of the sampled version of the complex baseband process $\nu_i(t)$ in Eq. (2). Thus, as shown in the Appendix, an effective maximization of the output signal-to-noise ratio can be achieved by minimization of the index given in Eq. (3) subject to the equality

$$\|\underline{w}\|^2 = K \tag{12}$$

for some constant K, or by simply minimizing the following index,

$$\sum_{j=1}^{k} |1 - \underline{w}^H(k)\underline{g}(j)|^2 + \gamma(k)(\|\underline{w}\|^2 - K) \tag{13}$$

with respect to $\underline{w}$ and $\gamma(k)$, where $\gamma(k)$ is the Lagrangian multiplier. Differentiation of Eq. (13) with respect to $\underline{w}$ yields the following constrained least-squares estimate for $\underline{w}$ in terms of $\gamma(k)$ as

$$\underline{\hat{w}}_{CLS}(k) = \left\{ \sum_{j=1}^{k} \underline{g}(j)\underline{g}^H(j) + \gamma(k) I \right\}^{-1} \sum_{j=1}^{k} g(j) \tag{14}$$

Substituting Eq. (14) into Eq. (12) yields an equation for the unknown $\gamma(k)$, which can be solved for $\gamma(k)$. Substituting $\gamma(k)$ back in Eq. (14) provides the constrained optimum solution for the weighting coefficient vector. Note, however, that there is no close-form solution for $\gamma(k)$ and, thus, some numerical optimization techniques may need to be applied to obtain $\underline{\hat{w}}_{CLS}$. A simplified solution is obtained by selecting some appropriate value for $\gamma(k)$ in Eq. (14) and then normalizing the estimate to have its norm equal to one. In an exponentially data-weighted version of Eq. (14), both the summands are multiplied by λ^{k-j} where λ is the exponential data-weighting coefficient. With these modifications, Eq. (14) has the following equivalent form.

$$\begin{aligned}
\underline{P}^{-1}(k) &= \lambda \underline{P}^{-1}(k-1) + \gamma_0 I + \underline{g}(k)\underline{g}^H(k) \\
\underline{\psi}(k) &= \lambda \underline{\psi}(k-1) + \underline{g}(k) \\
\underline{\hat{w}}(k) &= \underline{P}(k)\underline{\psi}(k) \\
\underline{\hat{w}}_{NLS} &= \underline{\hat{w}}(k)/\|\underline{\hat{w}}(k)\| \\
\gamma(k) &= \gamma_0(1-\lambda^k)/(1-\lambda)
\end{aligned} \tag{15}$$

Note that Eq. (15) requires a matrix inversion for each value of k for which $\underline{\hat{w}}(k)$ is desired. An approximate recursive form for Eq. (15), which does not require matrix inversion, may also be derived by applying the matrix inversion lemma. Note that in Eq. (15), the higher value of γ_0 results in the higher relative weight assigned to the noise variance at the combiner output. The initial values for $\underline{P}^{-1}$ and $\underline{\psi}$ at $k = 0$ may simply be selected equal to zero.

V. Least Squares Algorithm II

In an alternative solution, it may be assumed that the received focal plane signal is the result of the spatial convolution of the ideal signal (in the absence of any distortion) with an unknown filter response representing various distortions from all sources, including antenna surface deformations due to gravity, wind, antenna pointing errors, turbulence, etc., i.e.,

$$\underline{g}(k) = \underline{B}\,\underline{X}(k) + \underline{\nu}(k) \tag{16}$$

where $\underline{B}$ is a Toeplitz matrix, $\underline{X}$ is the focal plane signal vector that under appropriate sampling is equal to $[0 \ldots 010 \ldots 0]$ in the ideal case of plane-wave with no distortion, and $\underline{\nu}$ is the additive noise vector. The matrix $\underline{B}$ includes any distortion effects, pointing errors, etc. For the linear array case under consideration, $\underline{B}$ can be approximated by a circular matrix for large N or becomes identical to a circular matrix provided the vector $\underline{X}(k)$ and the signal vector $\underline{g}(k)$ are zero-padded. Thus, it is assumed that B is circular. In the absence of noise, it is observed that $\underline{X} = \underline{B}^{-1}\underline{g}$ where $\underline{B}^{-1}$ is also a circular matrix. However, $\underline{B}$ is unknown, and it needs to be estimated from the noisy observations. Or, more directly, $\underline{B}^{-1}$ is estimated as follows. Rewriting the model Eq. (16) as

$$\underline{X}(k) = \underline{F}^* \underline{g}(k) + \underline{\nu}(k); \quad k = 1, 2, \ldots \tag{17}$$

where $\underline{F}$ is an unknown circular matrix to be estimated from the given measurement $\underline{g}(k)$; $k = 1, 2 \ldots, n$. Letting

$\underline{f}^T = [f_1, f_2 \ldots f_N]$ denote the first row of the matrix $\underline{F}$, and $\underline{g}_\ell(k)$ denote the vector obtained by cyclically shifting $\underline{g}(k)$ right ℓ times, the following equivalent signal model is obtained.

$$\begin{bmatrix} 0 \\ 0 \\ \vdots \\ 1 \\ 0 \\ \vdots \\ 0 \end{bmatrix} = \begin{bmatrix} \underline{g}^T(k) \\ \underline{g}_1^T(k) \\ \vdots \\ \underline{g}_{N-1}^T(k) \end{bmatrix} \begin{bmatrix} f_1^* \\ f_2^* \\ \vdots \\ f_N^* \end{bmatrix} + \begin{bmatrix} v_1(k) \\ v_2(k) \\ \vdots \\ v_N(k) \end{bmatrix}; \quad k = 1, 2 \ldots \tag{18}$$

A least-squares estimate for $\underline{f}$ can be obtained from the signal model Eq. (18) and in its non-recursive form is given by

$$\hat{\underline{f}}(k) = \left\{ \sum_{j=1}^{k} \left(\sum_{\ell=0}^{N-1} \underline{g}_\ell(j) \underline{g}_\ell^H(j) \right) \right\}^{-1} \sum_{j=1}^{k} \underline{g}_{N/2}(j) \tag{19}$$

A recursive form for the estimate $\hat{\underline{f}}(k)$ may also be derived following the steps used in obtaining Eq. (11). Here recursion is over both the signal sample vector $\underline{g}(k)$ and its circular shifts. With appropriate initial values $\underline{P}(0,0)$ and estimate $\hat{f}(0,0)$, one has the following recursion in terms of the indices k and j, with k denoting time and j denoting the cyclic shift of the received signal vector,

$$\begin{aligned} \underline{P}(k,j) &= \lambda^{-1} \Big\{ \underline{P}(k,j-1) \\ &\quad - \left[\lambda + \underline{g}_{j-1}^H(k) \underline{P}(k,j-1) \underline{g}_{j-1}(k) \right]^{-1} \\ &\quad \times \underline{P}(k,j-1) \underline{g}_{j-1}(k) \underline{g}_{j-1}^T(k) \underline{P}(k,j-1) \Big\}; \\ &\qquad j = 1, 2, \ldots \\ \underline{P}(k+1,0) &= \underline{P}(k,N); \quad k = 1, 2, \ldots \\ \hat{\underline{f}}(k,j) &= \hat{\underline{f}}(k,j-1) + \underline{P}(k,j) \underline{g}_{j-1}(k) \\ &\quad \times \left[\xi_j - \underline{g}_{j-1}^H(k) \hat{\underline{f}}(k,j-1) \right]; \\ &\qquad j = 1, 2, \ldots \\ \hat{\underline{f}}(k+1,0) &= \hat{\underline{f}}(k,N); \quad k = 1, 2, \ldots \end{aligned} \tag{20}$$

where

$$\begin{aligned} \xi_j &= 1, \quad j = \lfloor N/2 \rfloor \\ &= 0, \quad j \neq \lfloor N/2 \rfloor \end{aligned}$$

where $\lfloor x \rfloor$ denotes the least integer greater than or equal to x for any real x. The circular spatial convolution of $\hat{\underline{f}}^*$ with the received signal $\underline{g}(k)$ yields the reconstructed signal vector $\underline{h}(k)$. In the case of perfect reconstruction (deconvolution), the central element of the vector $\underline{h}$ is the combined signal, while the remaining elements would be zero.

VI. Simulations

The performance of the least-squares algorithms of the previous section is presented here in terms of simulations. In the following simulations, a linear feed array is considered. For the purposes of these simulations, the received signal focal field is generated by spatially Fourier transforming a simulated linear aperture plane array. The signals in the simulated aperture are assumed to be of equal amplitude but with completely independent phase processes. Also, for the purposes of simulations, each of these phase processes is assumed to be a moving average process of a specified correlation interval K and variance (steady-state). The effectiveness of the different least-squares algorithms is measured in terms of the power ratio (in dB) of the reconstructed (combined) signal to the total received power (which would be concentrated in the central feed element under ideal conditions). In addition, the performance of the least-squares multi-element combining algorithm is compared against traditional single-element processing. It should be noted that for all of these simulation experiments, the noise variance at the combiner output is matched to the noise variance at the output of a single feed (the weighting parameter vector $\hat{\underline{w}}$ is normalized to have unit norm).

In the simulations reported here, it is assumed that the received signal is unmodulated with the signal field amplitude equal to 1 in the aperture plane, corresponding to a signal amplitude A_0 equal to 16 at the center feed in the focal plane (ideal case). In case of data modulation, a decision-directed approach may be used to remove the data modulation from the received signal. For the purposes of simulations, the sampling period is normalized to 1 sec. Thus, the variance σ^2 of the sampled complex envelope of the noise at any of the feed outputs used in the simulations is given by

$$\sigma^2 = A_0^2 / N_0 f_s \tag{21}$$

where f_s is the sampling frequency; N_0 is the one-sided noise spectral density; $P = A_0^2/2$ is the received-signal power; and the algorithm's performance is plotted as a function of the carrier-to-noise spectral density ratio: CNR $= (P/N_0)$ (in dB-Hz).

In Fig. 2, the reconstructed signal amplitude and phase estimates as a function of time measured in number of samples for the least-squares algorithm for a CNR of 10 dB-Hz are plotted. It may be observed from Fig. 2(a) that there is a considerable signal loss compared to the received signal amplitude equal to 16 for the ideal case. In the simulations, the initial estimate for the parameter vector $\hat{w}$ is selected to be $[\alpha \quad \alpha \ldots \alpha]$ with $\alpha = 1/16$. As is apparent from Fig. 2(b), the phase-estimation error of the reconstructed signal is much smaller compared to the rms phase error of 1 rad introduced in the simulated received signal field. Figure 3 plots the corresponding results for the modified least-squares algorithm for the same set of signal parameters and for $\gamma_0 = 100$. Comparison of Figs. 2(a) and 3(a) shows a very significant performance improvement due to the proposed modification of the least-squares algorithm. Results are plotted in Fig. 4 for the case of 20 dB CNR with the parameter γ_0 equal to 200. For this case, the signal amplitude and phase of the reconstructed signal are quite close to their respective values for the ideal case. The signal amplitude loss for this case is only 1.09 dB relative to the ideal case, and the rms phase error (after adaptive combining) is 0.1 rad.

A. Simulation Results for Least-Squares Algorithm I

Figure 5(a) plots the sample estimates of the signal power loss (compared to the ideal case) for the standard least-squares algorithm I. The signal loss P_L is simply computed as $P_L = 20\log_{10}(\hat{A}_{rms}/16)$ with

$$\hat{A}_{rms} = \sqrt{\frac{1}{M}\sum_{i=1}^{M}\hat{A}_i^2}$$

where $\hat{A}_i$ is the reconstructed signal amplitude at the ith sampling instance, and M is the number of sample values selected to be equal to 200 for these simulations. Figure 5(b) plots the signal estimation rms phase error $\hat{\Theta}_{rms}$ computed as

$$\hat{\Theta}_{rms} = \sqrt{\frac{1}{M}\sum_{i=1}^{M}\hat{\theta}_i^2}$$

where $\hat{\theta}_i$ is the phase of the combined signal at the ith sampling instance. It is apparent from these figures that although the least-squares algorithm is optimal with respect to the prediction error criterion, it is not satisfactory in terms of the signal-to-noise ratio of the combined signal. For the case of simulated phase dynamics, there is an asymptotic signal loss of 4 dB for the high CNR ($\sim$ 20 dB) case.

Figure 6 plots the performance of the modified least-squares algorithm with $\gamma_0 = 100$ and with the same set of signal parameters as for the case of Fig. 5. The results are computed for three different values of the weighting coefficient: λ equal to 0.925, 0.95, and 0.975. Comparison of Figs. 5(a) and 6 shows a dramatic improvement in performance due to the proposed modification. Thus, the asymptotic signal loss for this case and with $\lambda = 0.925$ is only 1.3 dB compared to a 4 dB loss for the standard least-squares algorithm. Increasing the value of γ_0 or reducing λ may further reduce the signal loss.

It is not difficult to understand this marked performance difference between the two algorithms. By minimizing the sum of the norm square of the estimated signal error and the noise variance of the combined signal output, the standard least-squares algorithm produces a relatively large noise variance at the output. This is so because at high CNR the contribution of noise to the total error is relatively much smaller than the contribution due to signal error (measured as a fraction of total signal), and, thus, the former is essentially ignored by the algorithm. In the constrained least-squares algorithm, by increasing the relative weighting attached to the noise variance, the signal-to-noise ratio at the combiner output is increased. In fact, as is shown in the Appendix, whereas the standard least-squares algorithm effectively maximizes the signal plus noise power output (subject to a near-orthogonality constraint), the constrained algorithm actually maximizes the signal-to-noise power ratio (subject to a similar near-orthogonality constraint) at the combiner output.

The signal loss results presented in Figs. 6(a)–(c) can also be used to infer the performance gains provided by the multi-element least-squares technique over center-feed processing. In particular, we can define the array processing gain as the difference (in dB) between the combining losses of the least-squares and center-feed curves. These data are plotted in Fig. 6(d).

As seen in Fig. 6(d), the array processing gain is a function of both CNR and λ. Best results occur for large CNR ($>$ 15 dB) and low values of λ ($\lambda = 0.925$). In par-

ticular, a maximum array gain of 3 dB (Fig. 6(a)) can be achieved for this simulation example. For lower values of CNR (below 0 dB), the estimation variance inherent in the least-squares algorithm degrades the array processing gain to such an extent that center-feed processing actually provides better performance.

However, it must be stressed that the simulation example considered here corresponds to a relatively high dynamic scenario, e.g., as compared with typical mechanically-induced array degradations. Lower dynamic scenarios permit longer time constants for the least-squares algorithm ($\lambda \rightarrow 1$ and/or longer sampling period), thereby reducing the algorithm estimation variance. Thus, for low dynamic scenarios, positive array gains can be achieved over a wider range of CNRs (including CNR $\ll 0$ dB) by utilizing time constants that are essentially matched to the dynamics. For sampling periods with T different from 1 sec, the results of Fig. 6 are applicable with the CNRs scaled by T. For instance, with $T = 10$ sec (typical for slower processes), the normalized CNR of 0 dB in Fig. 6 will correspond to the actual CNR of -10 dB.

It should also be noted that for a given scenario, increasing λ to such an extent that the algorithm cannot track the dynamics will lead to degraded system performance. This can be clearly seen from Fig. 6, where it is observed that the array gain for $\lambda = 0.975$ is approximately 1 dB less than for $\lambda = 0.925$. Finally, it can be observed from Fig. 7 that in contrast to the array gain results, there is little difference in rms phase error between the least-squares and center-feed outputs.

B. Simulation Results for Least-Squares Algorithm II

Figures 8(a) and (b) plot the performance of least-squares algorithm II in terms of signal reconstruction. In these figures, the dashed graphs depict the amplified signal amplitude A_i at the output of various feeds, while the solid-lined graphs represent the amplitude of the reconstructed field, i.e., the magnitude of various components of $\underline{h}(k)$ obtained by the circular convolution of the weight vector $\underline{\hat{f}}(k)$ obtained from Eq. (19) or Eq. (20), and the received signal vector $\underline{g}(k)$, for two different time indices equal to 30 and 185, respectively. As for the case of least-squares algorithm I, it is assumed that the weight vector $\underline{\hat{f}}$ is normalized to have its norm equal to 1. This ensures that the noise variance at various points of the reconstructed field is equal to the variance of the input noise field and, thus, the comparison in terms of signal amplitudes is equivalent to comparing the reconstructed signal-to-noise power ratio. The results in Fig. 8 correspond to the same set of signal parameters as for least-squares algorithm I and a CNR of 10 dB. As is apparent from Fig. 8, the least-squares algorithm II focuses most of the signal power that is originally dispersed in 16 taps into the center tap. A more appropriate measure of the effective focusing is obtained by the signal amplitude of the center tap of the reconstructed field, which is plotted versus time in Fig. 9(a). In this case, only -5.2 dB of the received signal power is scattered in the other taps for the reconstructed field. Figure 9(b) plots the phase error of the center tap signal and shows an rms phase error of 0.12 rad. Figure 10 plots the corresponding results for the case of $\gamma_0 = 100$ and differs insignificantly from the corresponding results in Fig. 9. Thus, the least-squares algorithm II simultaneously optimizes the signal-to-noise ratio. Figure 11(a) plots the signal loss in the center feed of the reconstructed signal for the least-squares algorithm II. As shown in the figure, with the parameter $\lambda = 0.925$, a loss of 1.25 dB can be achieved for the high CNR case, which is similar to that obtained for modified least-squares algorithm I. Figure 11(b) plots the corresponding results for the rms phase error of the reconstructed signal, showing an rms phase error of about 0.12 rad at CNRs higher than 10 dB.

Figure 12 plots the results when the algorithm is applied to a configuration of feeds connected to amplifiers with different noise figures. For this example, the case wherein one-half of the total number of amplifiers have 6.0 dB higher noise temperature than others is considered. The CNR in the figure is still measured with reference to the amplifier with the lower noise temperature. As may be inferred from Fig. 12(a), the asymptotic signal loss (CNR $>$ 10 dB) in this case is 2.2 dB as opposed to 1.2 dB for the case in which all of the amplifiers have low noise temperature, thus resulting in only 1 dB additional degradation. Note that if all the amplifiers were replaced by ones with higher noise temperature, then the degradation would be about 3 dB with reference to this lower CNR, thus resulting in an effective loss of 9 dB.

It may be remarked that in the above presentation, the sampling period T has been normalized to 1 sec, but the results are also applicable to different sampling periods by a simple normalization. As is apparent from Eq. (21), while increasing the sampling rate by a factor K, one should correspondingly reduce the actual CNR by the same factor to obtain the algorithm's performance for this case.

VII. Conclusions

From the simulations presented in the article, it can be observed that for the relatively fast distortion process

with a moderate dispersion and the array geometry considered, the multi-element array configuration provides an improvement of about 3 dB over a single-feed system. For a slower process with possibly higher spatial dispersion, the improvement is expected to be higher and to a certain extent will also be influenced by a match between the array geometry and the pattern of the received signal power dispersion.

Acknowledgments

The simulation model and the subroutine to generate the distorted phase process used in the simulation of the proposed algorithm were written by Victor Vilnrotter. The author thankfully acknowledges this and the discussion concerning the concept of deconvolution for this problem held with Victor Vilnrotter and George Zunich during this work.

References

[1] W. A. Imbriale et al., "Ka-Band (32-GHz) Performance of 70-Meter Antennas in the Deep Space Network," *TDA Progress Report 42-88*, vol. October–December 1986, Jet Propulsion Laboratory, Pasadena, California, pp. 126–130, February 15, 1987.

[2] J. W. Layland and J. G. Smith, "A Growth Path for Deep Space Communications," *TDA Progress Report 42-88*, vol. October–December 1986, Jet Propulsion Laboratory, Pasadena, California, pp. 120–125, February 15, 1987.

[3] S. J. Blank and W. A. Imbriale, "Array Feed Synthesis for Correction of Reflector Distortion and Vernier Beamsteering," *TDA Progress Report 42-86*, vol. April–June 1986, Jet Propulsion Laboratory, Pasadena, California, pp. 43–55, August 15, 1986.

[4] P. D. Potter, "64-Meter Antenna Operation at Ka-Band," *TDA Progress Report 42-57*, vol. March and April 1980, Jet Propulsion Laboratory, Pasadena, California, pp. 65–70, June 15, 1980.

[5] N. Mohanty, *Random Signals Estimation and Identification*, Van Nostrand Reinhold, New York, New York, 1986.

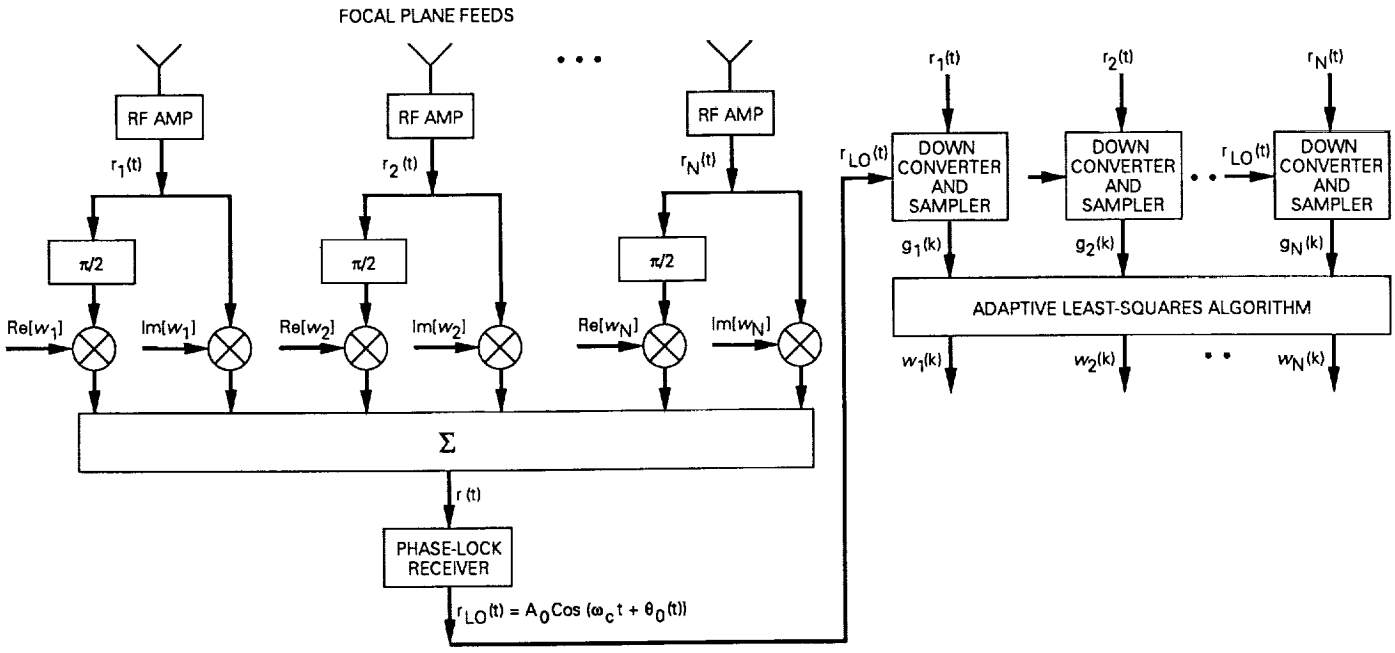

Fig. 1. RF signal combining in focal plane.

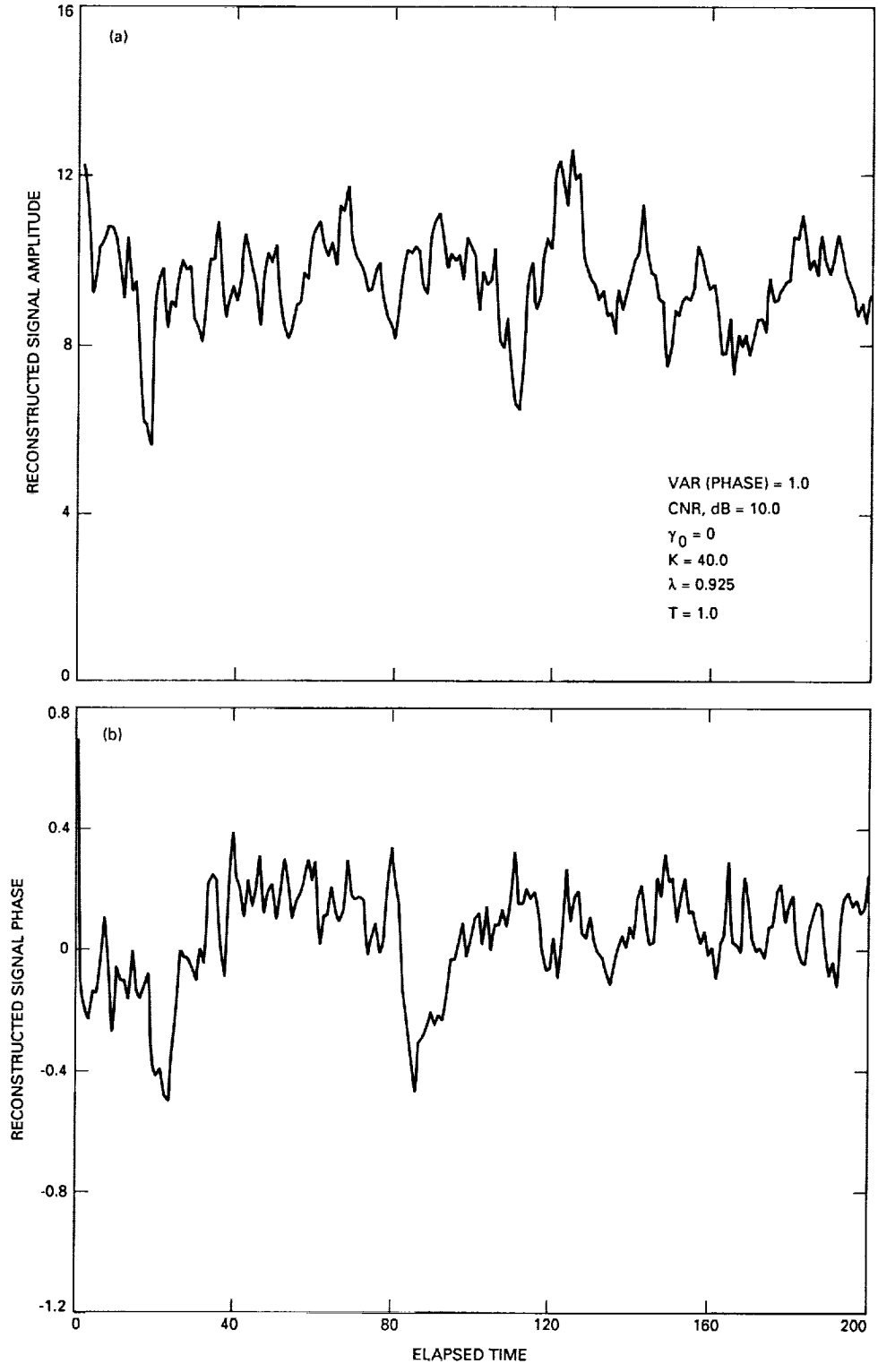

Fig. 2. Least-squares algorithm I: (a) reconstructed signal amplitude; (b) reconstructed signal phase.

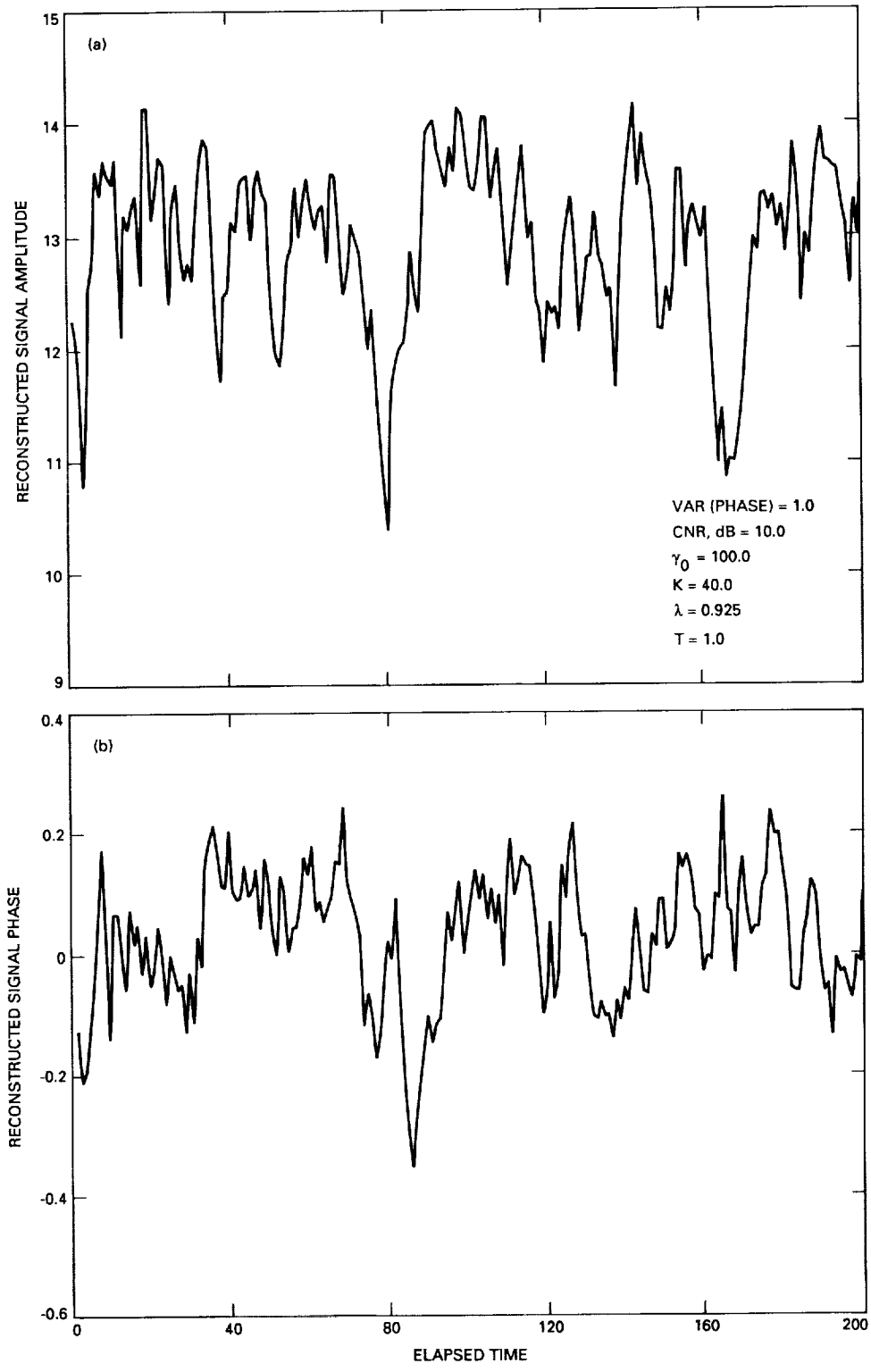

Fig. 3. Modified least-squares algorithm I: (a) reconstructed signal amplitude versus time; (b) reconstructed signal phase versus time.

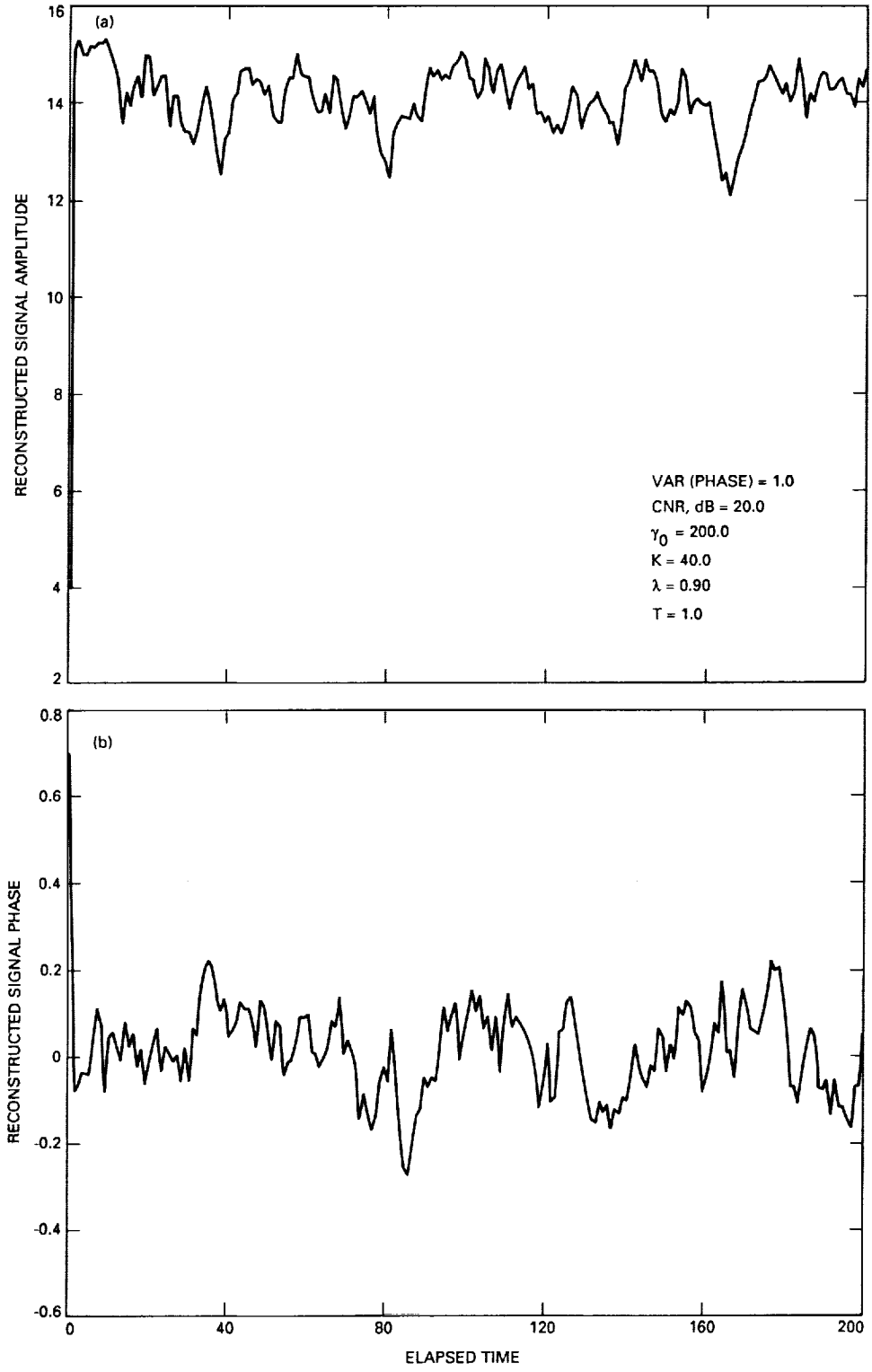

Fig. 4. Modified least-squares algorithm I: (a) reconstructed signal amplitude versus time at 20 dB CNR; (b) reconstructed signal phase versus time at 20 dB CNR.

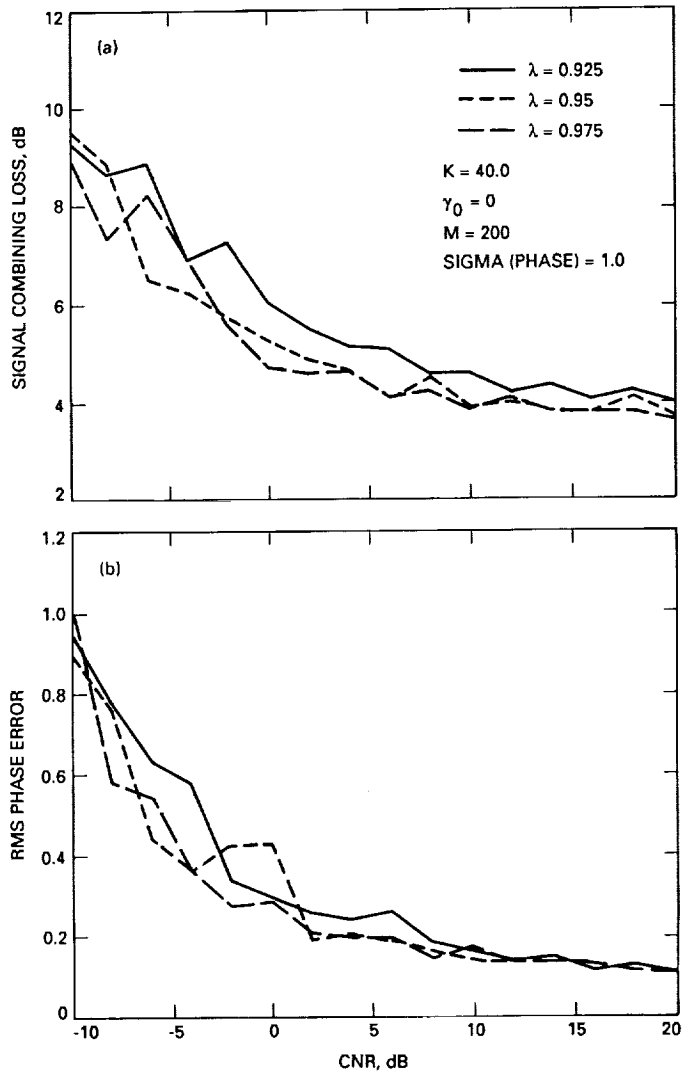

Fig. 5. Least-squares algorithm I: (a) signal combining loss versus CNR for reconstructed signal; (b) rms phase error versus CNR for reconstructed signal.

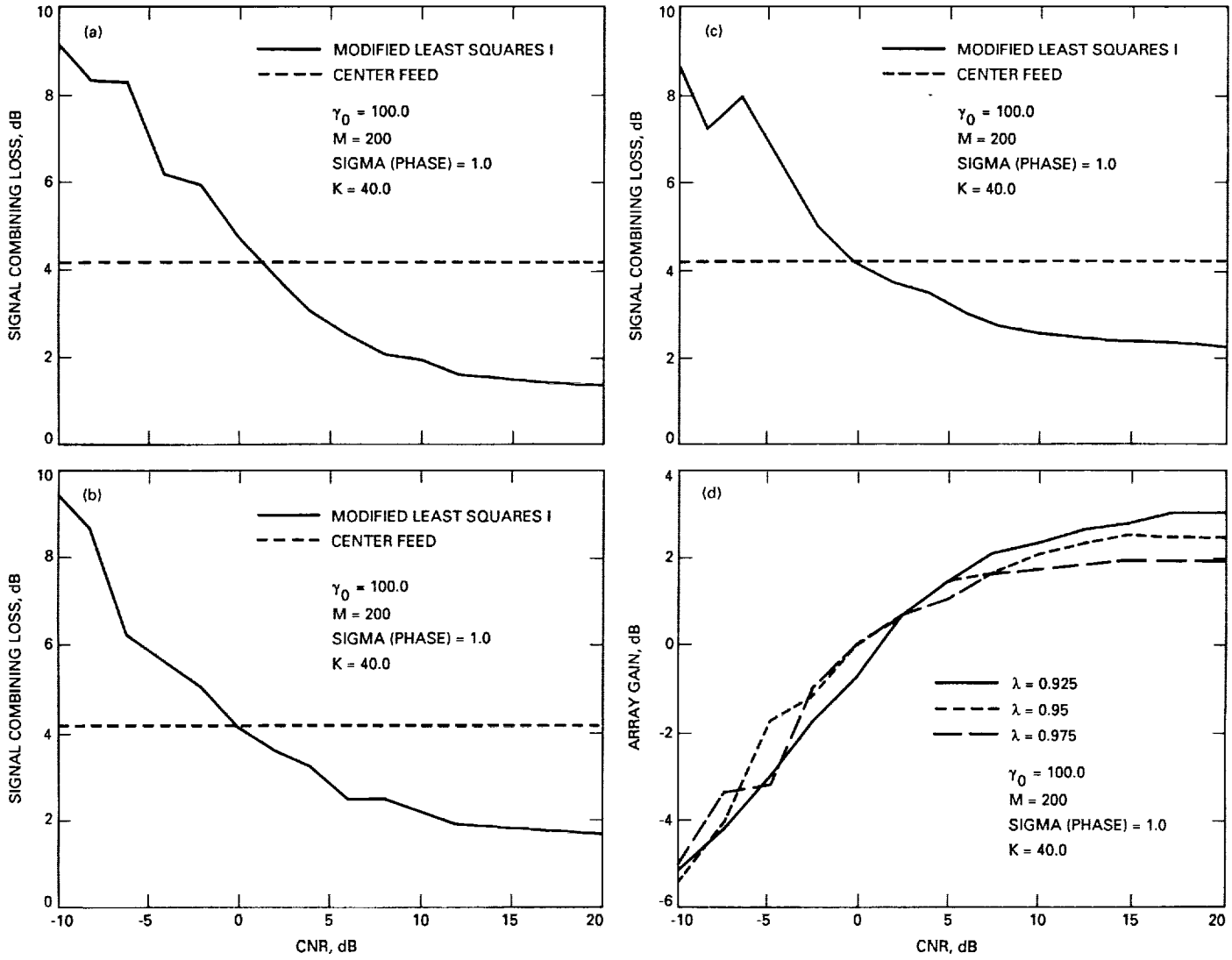

Fig. 6. Signal combining loss versus CNR for reconstructed signal: (a) $\lambda = 0.925$; (b) $\lambda = 0.95$; (c) $\lambda = 0.975$. Also (d) modified least-squares array gain versus CNR.

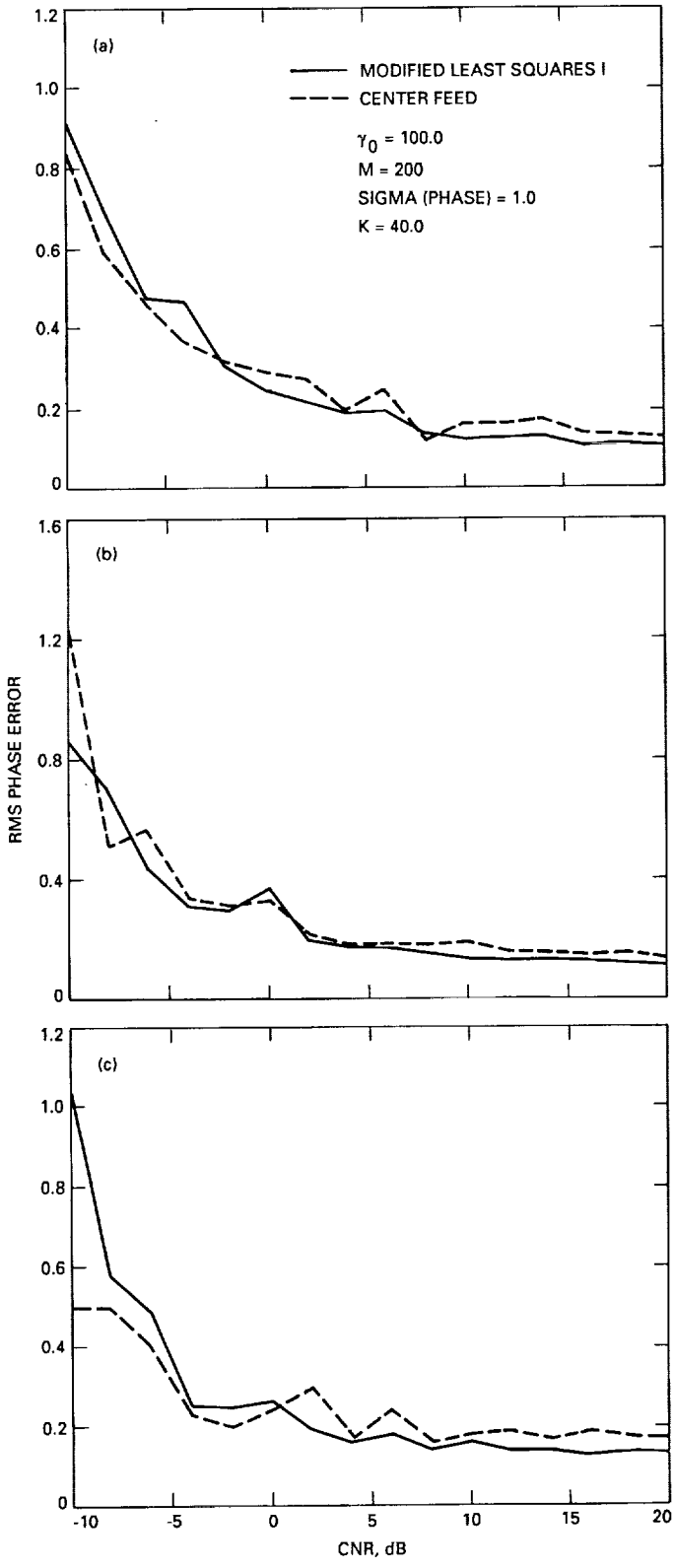

Fig. 7. rms phase error versus CNR for reconstructed signal: (a) $\lambda = 0.925$; (b) $\lambda = 0.95$; (c) $\lambda = 0.975$.

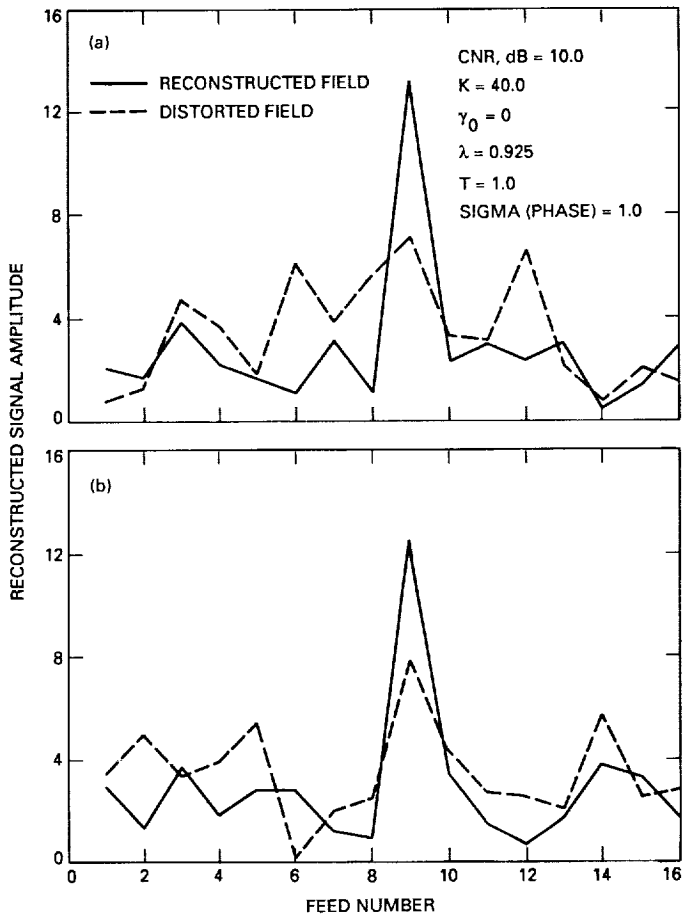

Fig. 8. Focal plane reconstructed field amplitude, least-squares algorithm II: (a) after 30 samples; (b) after 185 samples.

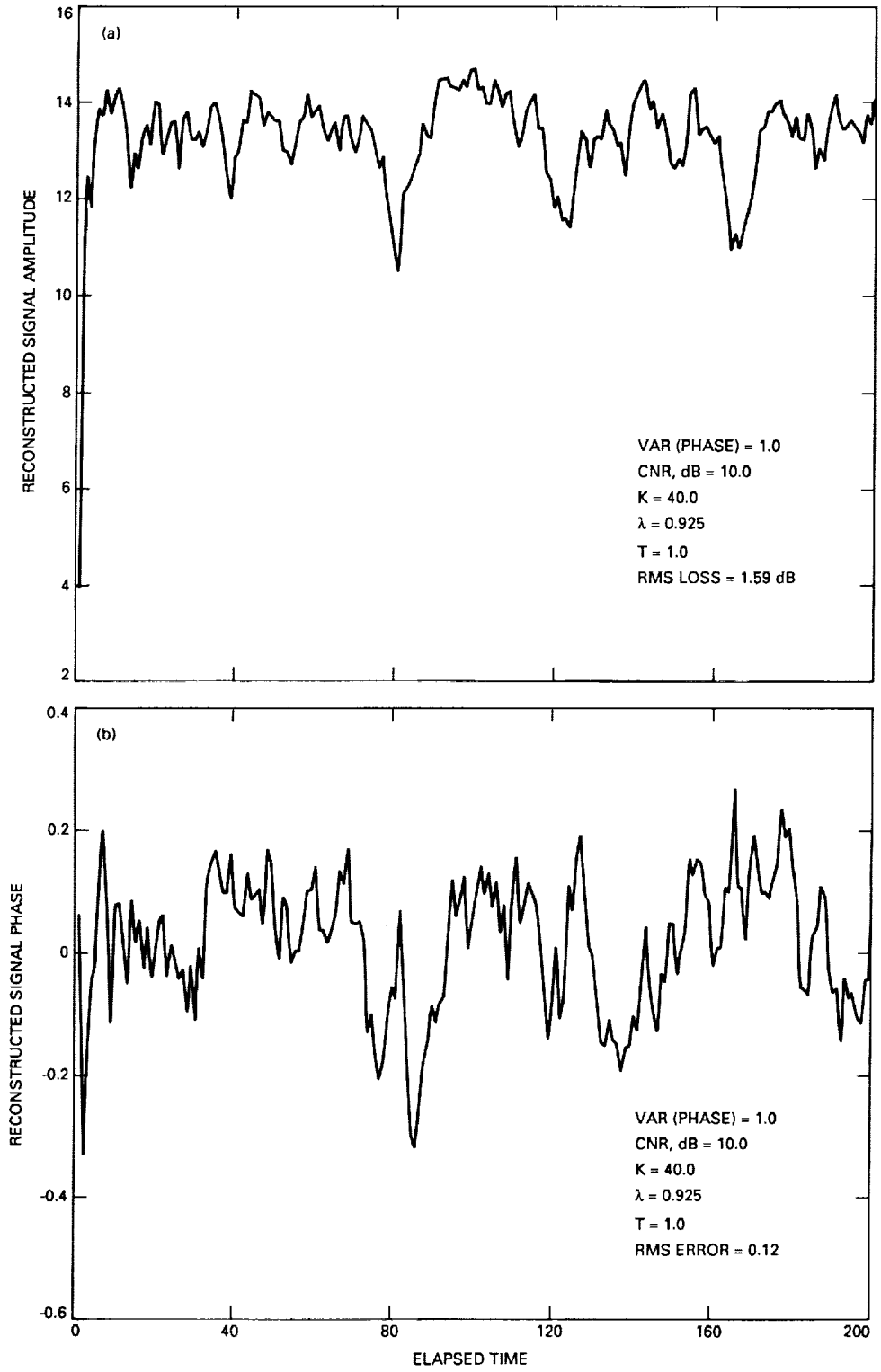

Fig. 9. Least-squares algorithm II: (a) focal plane reconstructed signal amplitude versus time, $\gamma_0 = 0$; (b) focal plane reconstructed signal phase versus time, $\gamma_0 = 0$.

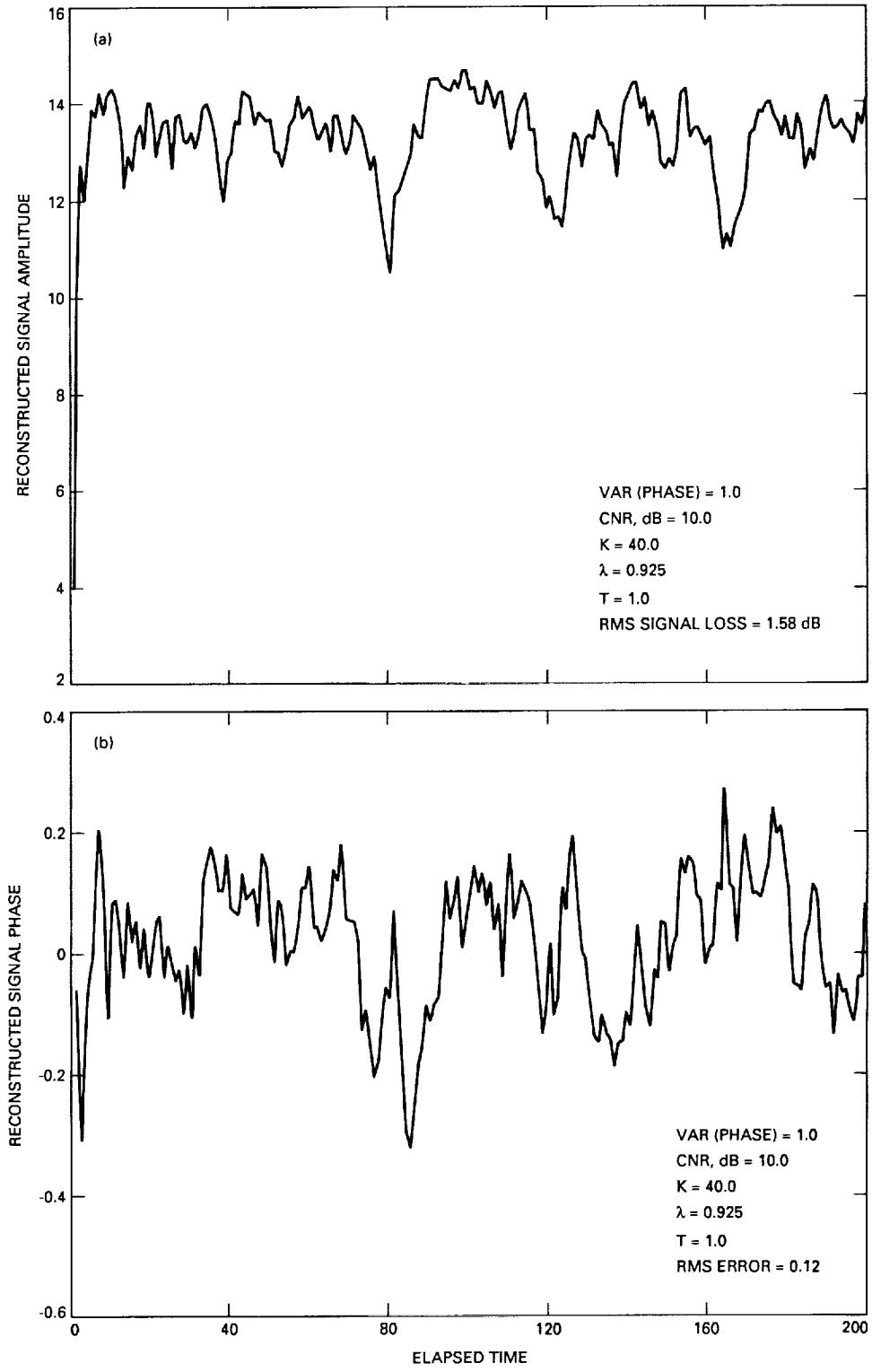

Fig. 10. Least-squares algorithm II, $\gamma_0 = 100$: (a) focal plane reconstructed signal amplitude versus time; (b) focal plane reconstructed signal phase.

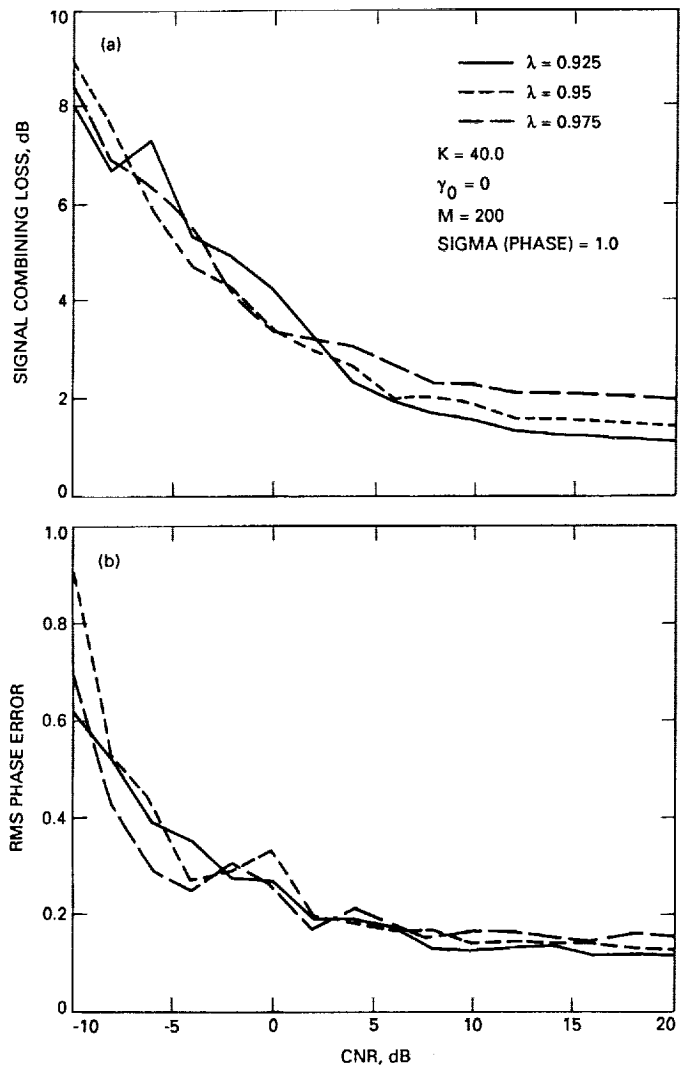

Fig. 11. Least-squares algorithm II: (a) signal combining loss versus CNR for reconstructed field; (b) rms phase error versus CNR for reconstructed field.

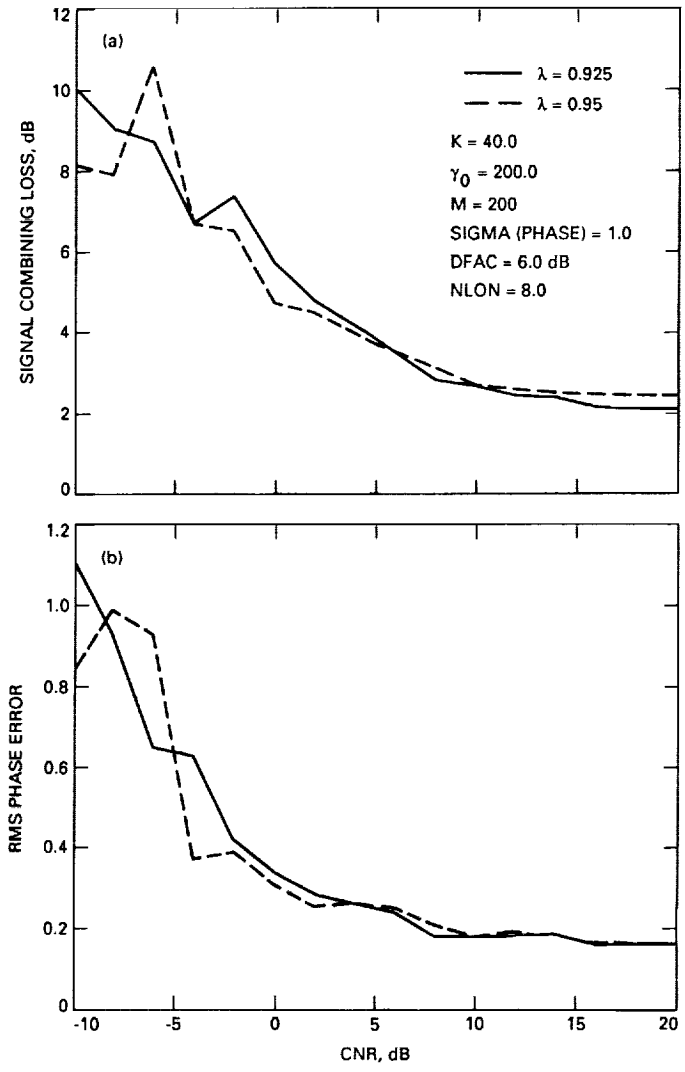

Fig. 12. Modified least-squares algorithm I, different noise figures: (a) signal combining loss versus CNR for reconstructed field; (b) rms phase error versus CNR for reconstructed field.

Appendix

The following shows that the modified least-squares algorithm I of Section IV achieves constrained maximization of the signal-to-noise ratio. In the first instance, the time averages are replaced by the ensemble averages.

Denoting by $s_i(k)$ the signal component of the ith array element output, consider the problem of minimizing

$$H = E\left[\left|S - \sum_{i=1}^{N} w_i^* s_i\right|^2\right] \tag{A-1}$$

with respect to $w_i, i = 1, 2, \ldots N$. Setting the partial derivative of H w.r.t.w_i to zero yields

$$E\left[\left(S - \sum_{i=1}^{N} w_i^* s_i\right) s_i^*\right] = 0 \tag{A-2}$$

Now with $\widehat{S} \triangleq \underline{w}^H \underline{s}$ and $\underline{s} \triangleq [s_1, s_2, \ldots, s_N]'$, the index H may be written as

$$E\left[|S - \widehat{S}|^2\right] = E\left[|S|^2 + |\widehat{S}|^2 - S\widehat{S}^* - S^*\widehat{S}\right] \tag{A-3}$$

At the optimal point, the following is obtained from Eq. (A-2).

$$E\left[(S - \widehat{S})\widehat{S}^*\right] = 0 \tag{A-4}$$

Adding the left-hand side of Eq. (A-4) and its complex conjugate to Eq. (A-3) yields the following form for the optimization index, subject to the constraint, Eq. (A-4).

$$H = |S|^2 - E\left[|\widehat{S}|^2\right] \tag{A-5}$$

Thus, the algorithm that minimizes Eq. (A-1) also maximizes $E\left[|\widehat{S}|^2\right]$, subject to the constraint, Eq. (A-4), i.e., it is also a signal maximization algorithm. There may also exist solutions that optimize $E\left[|\widehat{S}|^2\right]$ without the constraint, Eq. (A-4), but these may result in large phase error with respect to S, the desired signal, i.e., $\widehat{S}$ and $\widehat{S}e^{j\phi}$ (for any random phase ϕ) both have the same value of the index $E\left[|\widehat{S}|^2\right]$ but only one of these would simultaneously minimize the error function, Eq. (A-1). It may be remarked that there are, in general, an infinite number of solutions that satisfy Eq. (A-4), and in effect these orthogonalize the estimate $\widehat{S}$ and the "error" $(S - \widehat{S})$. Among these solutions, the one maximizing $E\left[|\widehat{S}|^2\right]$ is selected. Equation (A-4) is termed the orthogonality constraint.

The optimization index, Eq. (A-1), does not include the noise variance at the output of the array combiner, which is given by $\sigma^2 \|\underline{w}\|^2$ where σ^2 is the variance of $\nu_i(k)$, the noise at the input of the combiner. Thus, now Eq. (A-1) is minimized subject to the constraint

$$\|w\|^2 = K \tag{A-6}$$

for some constant K. Or, one can simply minimize

$$E\left[|S - \underline{w}^H \underline{s}|^2\right] + \beta\left(\|w\|^2 - K\right) \tag{A-7}$$

where β is the Lagrangian multiplier. An analysis similar to derivation of Eq. (A-5) shows that with a constraint similar to Eq. (A-4), the index is given by

$$|S|^2 - E\left[|\widehat{S}|^2\right] - 2\beta K \tag{A-8}$$

for some constants β and K. Thus, again the algorithm maximizes $E\left[|\widehat{S}|^2\right]$ subject to the constraint that the output noise variance is equal to a constant $K\sigma^2$, and thus effectively maximizes the output signal-to-noise ratio.

Now from the independence of the received signal s_i and noise ν_i it follows that

$$E\left[|S - \underline{w}^H \underline{g}|^2\right] = E\left[|S - \underline{w}^H \underline{s}|^2\right] + \|\underline{w}\|^2 \sigma^2 \tag{A-9}$$

Minimization of Eq. (A-9) subject to the constraint, Eq. (A-6), is thus identical to the minimization of Eq. (A-1) subject to the constraint, Eq. (A-6), and thus effectively maximizes the signal-to-noise ratio under the near orthogonality constraint. Now for the large value of k, the index $k^{-1}J_k$ with J_k given by Eq. (3) approaches the left-hand side of Eq. (A-9) under appropriate ergodicity assumptions, and the algorithm of Section IV thus achieves constrained optimization of the signal-to-noise power ratio.

It may be remarked that the least-squares algorithm in the absence of the constraint, Eq. (A-6), effectively minimizes the following index

$$|S|^2 - E\left[|\widehat{S}|^2\right] - \sigma^2\|\underline{w}\|^2 \qquad \text{(A-10)}$$

subject to a constraint similar to Eq. (A-4). Since the last term in Eq. (A-10) represents the noise power at the combiner output, it can be observed that the standard least-squares algorithm effectively maximizes the sum of the signal plus noise power rather than the signal-to-noise power ratio.